Organic Geochemistry 132 (2019) 37–49

Contents lists available at ScienceDirect

Organic Geochemistry

journal homepage: www.elsevier.com/locate/orggeochem

The vertical distribution of Thaumarchaeota in the water column of Lake Malawi inferred from core and intact polar tetraether lipids

Dervla Meegan Kumar [a,b], Martijn Woltering [c,d], Ellen C. Hopmans [e], Jaap S. Sinninghe Damsté [e,f], Stefan Schouten [e,f], Josef P. Werne [a,c,*]

[a] Department of Geology and Environmental Science, University of Pittsburgh, Pittsburgh, PA 15260, USA
[b] Department of Geosciences, University of Arizona, Tucson, AZ 85719, USA
[c] Large Lakes Observatory, University of Minnesota Duluth, 10 University Dr., Duluth, MN 55812, USA
[d] CSIRO Earth Science and Resource Engineering, Australian Resources Research Centre, Kensington, Perth, WA 6151 Australia
[e] NIOZ Royal Netherlands Institute for Sea Research, Department of Marine Microbiology and Biogeochemistry, and Utrecht University, PO Box 59, 1790 AB Den Burg, Texel, the Netherlands
[f] Department of Geosciences, Utrecht University, Budapestlaan 4, 3584 CD Utrecht, the Netherlands

ARTICLE INFO

Article history:
Received 17 December 2018
Received in revised form 12 March 2019
Accepted 19 March 2019
Available online 19 March 2019

Keywords:
TEX_{86}
Thaumarchaeota
GDGT
Intact polar lipids
Lake Malawi

ABSTRACT

Several long paleoclimate records generated from Lake Malawi sediments rely on an assumption that the TEX_{86} paleothermometer reflects annual mean lake surface temperatures. Thaumarchaeota, the producers of the isoprenoid glycerol dialkyl glycerol tetraether (iGDGT) lipids that are the basis of the TEX_{86} proxy, can occupy a wide range of habitats in the upper water column of lacustrine systems, so it is crucial to specifically constrain the ecology of Thaumarchaeota in Lake Malawi to properly interpret its sedimentary TEX_{86} record. To investigate the spatial and vertical distribution of Thaumarchaeotal iGDGT production in Lake Malawi, suspended particulate matter (SPM) was collected from the upper water column (>300 m) at three sites spanning the north, central, and south basins of the lake and analyzed for intact polar (IPL) and core (CL) iGDGT lipid abundances. Samples were collected in January during the austral summer when the lake is strongly stratified. Concentrations of the most labile IPL, hexose-phosphohexose (HPH)-crenarchaeol, were greatest just below the deep chlorophyll maximum at ~50 m water depth in the deeper north and central basins and ~30 m in the shallow south basin. Maximum CL concentrations occur below the maximum HPH-crenarchaeol concentrations and therefore possibly reflect the accumulation of recently produced IPL GDGT degradation products. If the export of CLs to the sediments is dominated by this CL pool, sedimentary TEX_{86} would reflect Thaumarchaeota living within the thermocline during the stratified season and therefore may have a cool bias rather than reflecting true surface water temperatures. An increase in abundances of GDGT-2, crenarchaeol isomer, and monohexose (MH)-crenarchaeol at ~150–200 m suggests that a secondary Thaumarchaeotal population, likely Group I.1b Thaumarchaeota, inhabits the subsurface water column near the anoxic-suboxic boundary. Total production of iGDGTs by this group appears to be much lower than the surface-dwelling clade, but its imprint on sedimentary TEX_{86} is unknown. An analysis of iGDGT production in the water column throughout the annual cycle is needed to resolve the timing and magnitude of export of CLs to the sediments from these two Thaumarchaeotal populations.

1. Introduction

Terrestrial climate can be difficult to characterize due to its inherent heterogeneity, though the omnipresence of lakes across the continents provides a means for reconstructing a mosaic of local- to regional-scale responses to climate perturbations. Lake sediments are ideal for multi-proxy analyses as they contain signals of both in situ and terrestrial processes integrated within their drainage basins. It is crucial that paleotemperature reconstructions are generated alongside multi-proxy records to provide a unifying context through which the local response to climatic change can be evaluated across spatially distributed basins. Certain classes of lipids preserved in sediments can be used for terrestrial paleotemperature reconstructions if they are ubiquitous in lacustrine sys-

* Corresponding author.
E-mail address: jwerne@pitt.edu (J.P. Werne).

https://doi.org/10.1016/j.orggeochem.2019.03.004
0146-6380/

tems and their distributions are quantitatively related to environmental temperatures.

Isoprenoid glycerol dialkyl glycerol tetraethers (iGDGTs) are one such class of lipids. Distributions of iGDGTs are described in the TEX_{86} proxy (Schouten et al., 2002), which has been demonstrated to correlate to lake surface temperatures (LST) in some systems (e.g., Blaga et al., 2009; Bechtel et al., 2010). The relationship between TEX_{86} and water temperature is founded on the premise that mesophilic Thaumarchaeota (called Group I Crenarchaeota in earlier studies; Brochier-Armanet et al., 2008; Spang et al., 2010) retain the ability to increase production of iGDGT membrane lipids containing cyclopentane moieties (Fig. 1) in response to increasing growth temperatures (Schouten et al., 2002; Wuchter et al., 2004; Elling et al., 2015), a process previously believed to be exclusive to their (hyper)thermophilic ancestors (Gliozzi et al., 1983). The cyclization of iGDGTs enhances the rigidity of the cell membrane and thus the addition of cyclopentane moieties is widely accepted as a biophysical adaption of Archaea to ambient water temperatures (Schouten et al., 2013 and References cited therein).

The relationship between TEX_{86} and LST is generally strongest in large oligotrophic lakes (Blaga et al., 2009; Powers et al., 2010; Tierney et al., 2010); as such, the large rift lakes of east Africa are ideal sites for TEX_{86}-based paleothermometry. Indeed, plausible paleotemperature records have been generated with TEX_{86} in sediments from Lakes Malawi (Powers et al., 2005, 2011; Woltering et al., 2011; Johnson et al., 2016), Tanganyika (Tierney et al., 2008, 2010), Victoria (Berke et al., 2012a, 2012b), Turkana (Berke et al., 2012a, 2012b; Morrissey et al., 2018), Albert (Berke et al., 2014), and Challa (Sinninghe Damsté et al., 2012a). Whether the

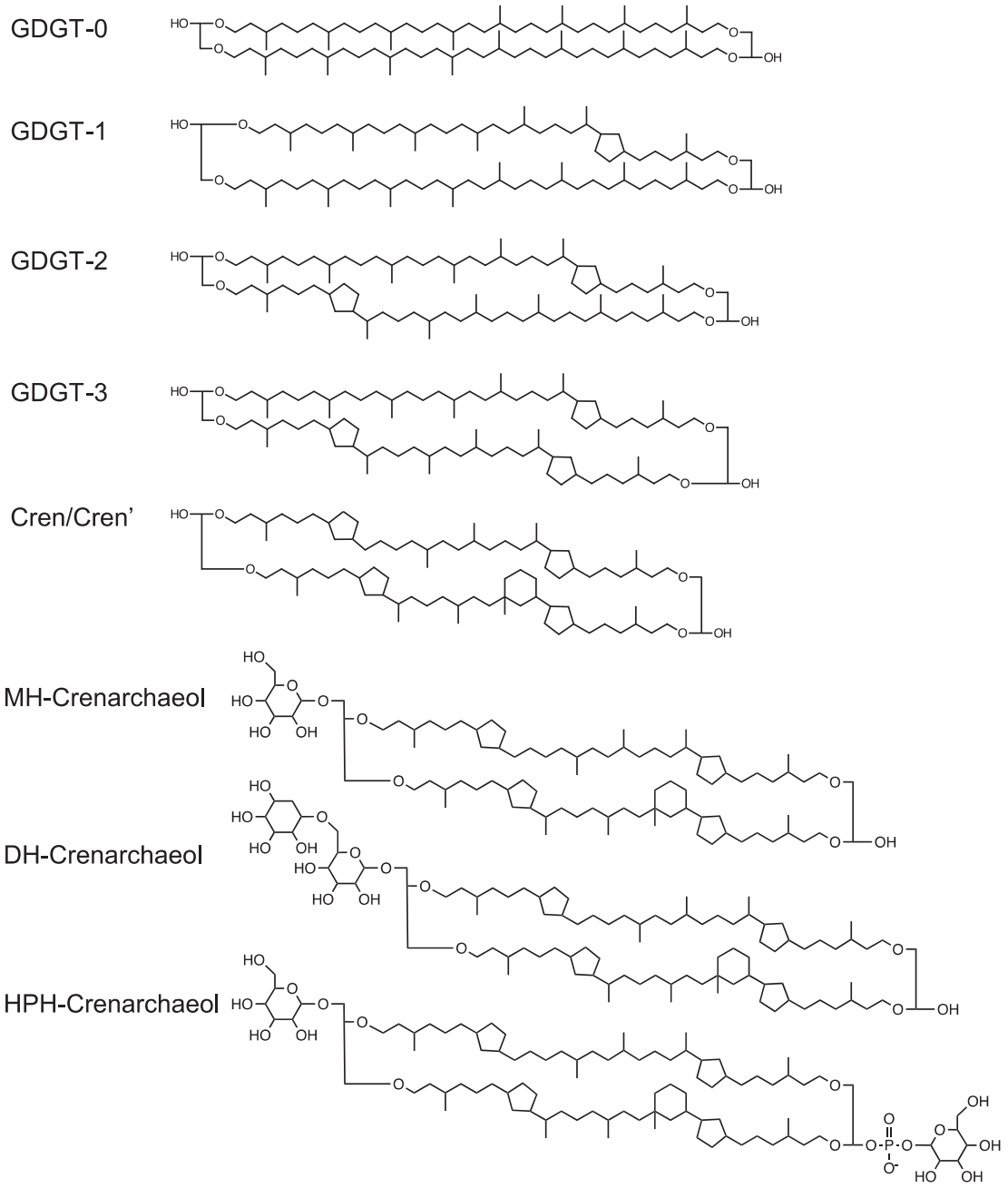

Fig. 1. Molecular structures of archaeal iGDGT core lipids (CL) and crenarchaeol intact polar lipids (IPL) with monohexose (MH), dihexose (DH), and hexose-phosphohexose (HPH) headgroups.

downcore TEX_{86} values in these basins consistently reflect LST, however, hinges on two assumptions: (1) iGDGTs are produced in the surface waters, and (2) Thaumarchaeota are the primary source of sedimentary iGDGTs. Previous studies of iGDGTs in the modern water column of some of the aforementioned lakes indicate that these assumptions may not necessarily be correct, or constant through time (Sinninghe Damsté et al., 2009; Llirós et al., 2010; Schouten et al., 2012a; Buckles et al., 2013, 2014; Villanueva et al., 2014a, 2014b). Variability in the depth and seasonality of iGDGT production among lakes may explain some of the scatter observed in current lacustrine TEX_{86} calibrations (Blaga et al., 2009; Powers et al., 2010; Tierney et al., 2010; Castañeda and Schouten, 2011, 2015; Kraemer et al., 2015). These parameters are therefore necessary to constrain within individual systems in order to properly evaluate sedimentary TEX_{86}-based paleotemperature reconstructions.

In this study, we measured both core (CL) and intact polar (IPL) iGDGT lipids in suspended particulate matter (SPM) at three sites in Lake Malawi. IPL GDGTs can track living populations of Archaea due to their labile nature, while refractory CLs are preserved on longer time scales (Sturt et al., 2004; Lipp et al., 2008; Lipp and Hinrichs, 2009; Liu et al., 2011; Pitcher et al., 2011a, 2011b). Using this divergence, we will attempt to constrain the vertical distribution of Thaumarchaeota and iGDGT production in Lake Malawi's water column with the goal to improve the interpretation of sedimentary TEX_{86} signals.

2. Materials and methods

2.1. Lake Malawi

Lake Malawi is the southernmost of the East African Rift Lakes (Fig. 2). It is a large (560 km long, up to 75 km wide, and over 700 m deep; Eccles, 1974; Johnson and Davis, 1989) meromictic rift lake in the southern hemisphere tropics (extending from ~9°S to 14°S). The water column is permanently anoxic below ~200 m, although the anoxic hypolimnion does not extend over the whole length of the lake and an extensive area in the shallower southern basin remains well-oxygenated year-round.

The limnology and ecology of Lake Malawi are heavily influenced by the movements of the Intertropical Convergence Zone (ITCZ). The lake is located at the southern terminus of the ITCZ's annual migration, resulting in a monsoon-like climate with only one rainy season that occurs during the austral summer (November–March). During the wet summer season, the dominant winds are weak and come from the north due to the position of the ITCZ directly over the lake. The weak northerly winds coupled with high seasonal insolation promotes stratification of the upper water column to ~50 m. The rainy season is followed by an 8 month long dry season during which many ephemeral rivers that empty into the south basin cease flowing (Beadle, 1981; Hamblin et al., 2003b). As the ITCZ migrates northward beginning in April, persistent strong southerly winds drive physical mixing in the upper 200 m that results in a breakdown of the summer stratification and a deepening of the thermocline (Eccles, 1974). In September easterly winds with reduced strength relative to the winter southerlies prevail, allowing for a relaxation of the mixing regime during austral springtime and the initiation of surface water stratification (Eccles, 1974).

2.2. Sampling

Sampling of SPM in Lake Malawi's water column was performed at three locations covering the lake's north, central, and south basins from the R/V Ndunduma over January 9–13, 2010 (Fig. 2). The north basin site (NB) (10°01′06.0″S, 34°11′12.0″E, 350 m water depth) was selected to correspond with the location of the MAL05-2A drill core, which contains a 70 ky record of TEX_{86} (Woltering et al., 2011). The central basin site (CB) (11°17′42.0″S, 34°26′12.0″E, 600 m water depth) coincides with the location of the MAL05-1C drill core that is the basis of a 1.3 million year paleotemperature record, also generated with the TEX_{86} temperature proxy (Johnson et al., 2016), and

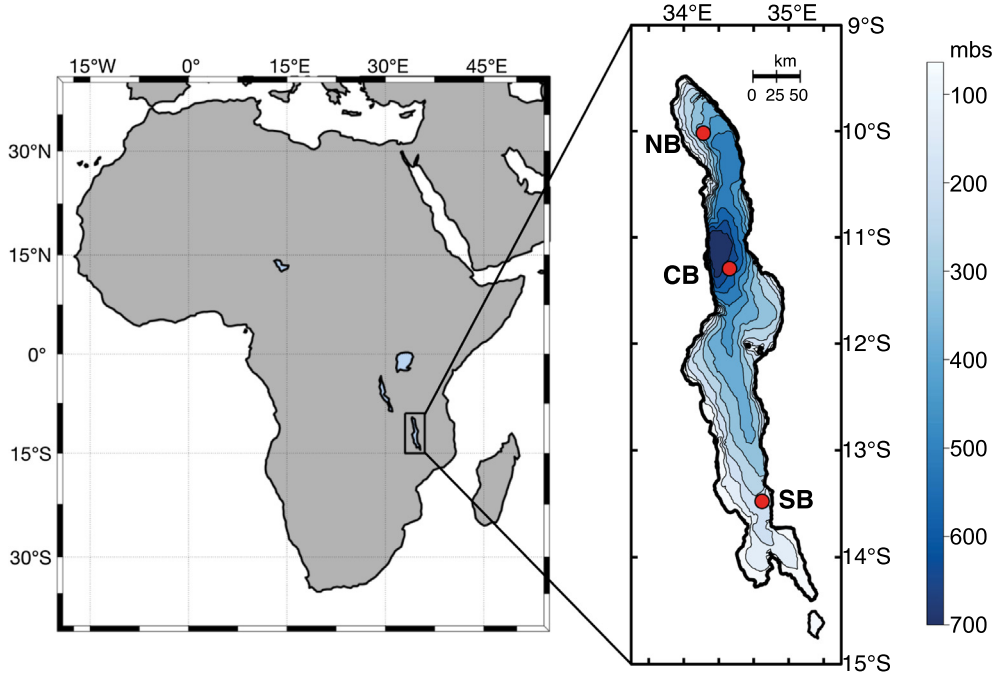

Fig. 2. Lake Malawi in geographic context of the African continent and its bathymetry. Sampling locations are indicated on the bathymetry map, where NB = North Basin, CB = Central Basin, and SB = South Basin. Bathymetry colour scale refers to water depth in meters below lake surface (mbs) (data were contoured by Thomas C. Johnson and Barbara M. Halfman, and digitized by Paul Cooley).

is proximal to the northernmost site of an earlier sediment trap study (Lake Malawi Biodiversity Conservation Project/LMBCP; Bootsma and Hecky, 1999). The south basin site (SB) (13°28′42.0″ S, 34°44′48.0″E, 175 m water depth) is located near the southern trap from the LMBCP and was also studied extensively in a previous effort to characterize the ecology and limnology of Lake Malawi (Station 900 of Bootsma and Hecky, 1999).

Water column profiles of temperature, dissolved oxygen (DO), and chlorophyll-a concentrations were obtained with a SeaBird Model 19® plus CTD with fluorometer, DO, pH, and water pressure sensors. SPM for lipid analyses was collected with a McLane 6-1-142LV in situ filtration system. Samples were taken at seven depths at NB and CB and at four depths at SB, effectively covering the epilimnion and metalimnion at each location. Water samples (250–500 L at each depth) were filtered through 142 mm diameter 0.7 μm nominal pore size glass fiber filters. All filters were stored frozen in a block of ice onboard the ship, then transported from Malawi to the University of Minnesota Duluth (UMD) frozen in ice, and upon arrival at UMD were stored frozen until analyzed.

2.3. GDGT extractions

The glass fiber filters containing SPM were freeze dried, cut into small pieces, and extracted using a modified Bligh-Dyer technique (Bligh and Dyer, 1959; Sturt et al., 2004). The samples were ultrasonically extracted three times using dichloromethane (DCM)/methanol (MeOH)/0.1 M phosphate buffer (PB) (2:1:0.8, v/v/v) at pH = 7.4. The combined extracts were adjusted to a solvent ratio of DCM/MeOH/PB of 1:1:0.9 (v/v/v) and centrifuged to achieve phase separation, after which the DCM phase containing the organic material was collected and transferred to a clean vial. This extraction was repeated twice with fresh DCM and all DCM phases were combined. The resulting Bligh-Dyer extracts (BDEs) were split into aliquots for separate IPL and CL analyses. The aliquots intended for analysis of CL GDGTs were separated into apolar and polar fractions with alumina column chromatography, using hexane/DCM (9:1, v/v) to elute the apolar fraction and DCM/MeOH (1:1, v/v) to elute the polar fraction. A known amount (0.1 μg) of a C_{46} glycerol trialkyl glycerol tetraether internal standard (Huguet et al., 2006) was added to each of the polar fractions and evaporated under N_2 gas until dry. Just before analysis, the polar fractions were re-dissolved in hexane/isopropanol (99:1, v/v) to a concentration of 2 mg mL^{-1} and filtered over a 0.45 μm PTFE filter.

2.4. HPLC analyses

CL GDGTs from the polar fractions were analyzed via high performance liquid chromatography–positive ion atmospheric pressure chemical ionization mass spectrometry (HPLC–APCI-MS), using selected ion monitoring (SIM) of the $[M + H]^+$ protonated molecules on an Agilent 1100 HPLC–MS with an Alltech Prevail Cyano Column (150 × 2.1 mm, 3 μm) following the methods described in Schouten et al. (2007).

The analysis of monohexose (MH) crenarchaeol, dihexose (DH) crenarchaeol, and hexose phosphohexose (HPH) crenarchaeol IPLs (Fig. 1) was performed with an HPLC–electrospray ionization (ESI)–MS-MS in selected reaction monitoring (SRM) mode on an Agilent 1100 series LC, equipped with a thermostat-controlled autoinjector and column oven coupled to a Thermo TSQ Quantum Ultra EM triple quadrupole mass spectrometer with an Ion Max source and an ESI probe (Pitcher et al., 2011b). Separation was achieved with a Lichrosphere diol column (250 × 2.1 mm; 5 μm particles; maintained at 30 °C). A flow rate of 0.2 mL min^{-1} and the following linear gradient was used: 100% eluent A to 35% eluent A/65% eluent B over 45 min, which was maintained for 20 min, and then back to 100% eluent A for 20 min to re-equilibrate the column, where eluent A is hexane/isopropanol/formic acid/14.8 M $NH_{3(aq)}$ (79:20:0.12:0.04, v/v/v/v) and eluent B is isopropanol/water/-formic acid/14.8 M $NH_{3(aq)}$ (88:10:0.12:0.04, v/v/v/v). The ESI settings were as follows: capillary temperature 250 °C; sheath gas (N_2) pressure 49 arbitrary units; auxiliary gas (N_2) pressure 21 arbitrary units; spray voltage 4.2 kV; and source collision-induced dissociation −14 V. The SRM transitions were optimized according to Pitcher et al. (2011b). Due to a lack of available quantitative standards, IPL concentrations are reported as peak area (PA) response per liter of water filtered.

3. Results

3.1. Water column conditions

Water column properties were measured during the collection of SPM in January at the peak of summer stratification. Temperatures of surface waters were similar across the lake, 28.6 °C at NB, 28.8 °C at CB, and 28.4 °C at SB. The deeper northern and central basins exhibited many similarities. The thermocline began ~40 m at both NB and CB, with water temperatures decreasing to 23 °C by 70 m at NB, and by 100 m at CB (Fig. 3). Chlorophyll-a concentrations show a deep chlorophyll maximum situated at the top of the thermocline of both sites (Fig. 3). DO ranged from oversaturation in the epilimnion to <30% saturation by 145 m at NB and by 120 m at CB, and anoxic conditions persist below 200 m at both locations (Fig. 3). The upper stratified layer at SB extended to only 22 m and water temperatures decreased by ~4 °C in the thermocline, dropping below 24 °C by ~80 m. Chlorophyll-a concentrations at SB also indicate a deep chlorophyll maximum at the time of sampling, however, situated deeper within the thermocline at this site, ~30–35 m, rather than at the top of the thermocline as at NB and CB. The entire water column at SB was fully oxygenated, though the degree of oxygen saturation declined below 30 m towards ~72% at the deepest sampling point.

A previous study defined the epilimnion, metalimnion, and hypolimnion of Lake Malawi based on the exchange time of chemical tracers between water masses (Vollmer et al., 2002). As our study only examines the upper 300 m of the lake, we will instead define qualitative boundaries specific to the study period to provide clarification for the discussion below. Based on the parameters above, we define "surface" waters as the nearly isothermal layer above the top of the thermocline, 0–40 m at NB and CB and 0–22 m at SB, such that the "subsurface" includes all points below. The subsurface is further divided into "thermocline depths" that encompass 40–100 m at NB and CB and 22–100 m at SB, and the "deep subsurface" refers to all depths >100 m.

3.2. Crenarchaeol IPL abundances

Concentrations of all three crenarchaeol IPLs (Fig. 1) were 1–3 orders of magnitude lower in the surface than in the subsurface (Fig. 4; Table 1). The depth of maximum concentrations varied for the different head groups and by site. Maximum abundances of HPH-crenarchaeol occur at 50 m at NB (9.4×10^4 peak PA L^{-1}) and CB (9.2×10^5 PA L^{-1}), and at 30 m at SB (6.3×10^4 PA L^{-1}). NB contains a single maximum in DH-crenarchaeol concentrations at 100 m (1.3×10^5 PA L^{-1}), whereas DH-crenarchaeol concentrations show maxima at 50 m (1.1×10^5 PA L^{-1}) and 150 m (1.3×10^5 PA L^{-1}) at CB. Concentrations of MH-crenarchaeol peak twice at NB and CB, at 100 m (2.5×10^5 PA L^{-1})/200 m (3.3×10^5 - PA L^{-1}) and 50 m (3.2×10^5 PA L^{-1}) /200 m (2.2×10^5 PA L^{-1}), respectively. At SB, DH- and MH-crenarchaeol concentrations increased steadily with depth, reaching maximum concentrations

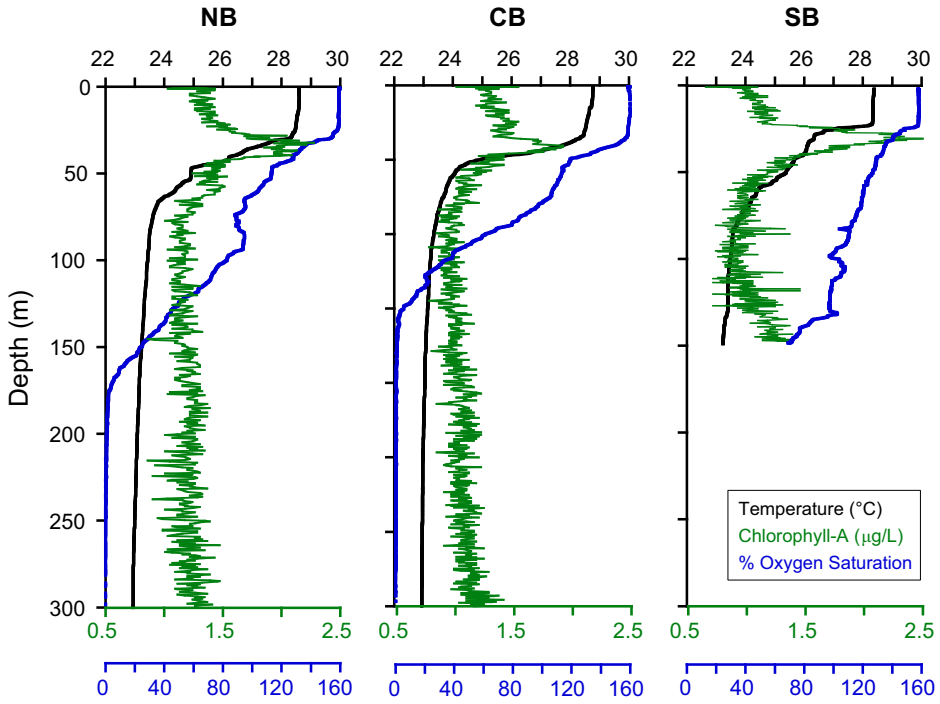

Fig. 3. CTD measurements of temperature, chlorophyll-a, and dissolved oxygen in Lake Malawi in January 2010. Though the water column does extend beyond 300 m in the northern and central basins, the deep subsurface was not measured for this study.

at 150 m (1.2×10^5 PA L^{-1} and 5×10^5 PA L^{-1}, respectively). The highest total IPL abundance (1.4×10^6 PA L^{-1}) was observed at CB due to concentrations of HPH-crenarchaeol that were an order of magnitude greater than at NB or SB.

3.3. GDGT concentrations

Concentrations of the Thaumarchaeota biomarker, crenarchaeol (Sinninghe Damsté et al., 2002), ranged from 0.03 to 40.3 ng L^{-1} (Table 1). SPM from the surface waters at all three sites contained the lowest concentrations of crenarchaeol. Crenarchaeol concentrations peaked at 100 m at NB (30.7 ng L^{-1}) and CB (37.1 ng L^{-1}), and at 150 m at SB (40.3 ng L^{-1}), well below the thermocline in each location (Fig. 4; Table 1). Though concentrations of GDGTs 0–3 were an order of magnitude lower than crenarchaeol, their vertical profiles showed generally similar trends with peaks in abundance near 100 m for NB and CB, and at 150 m for SB. Significant departures from this trend were observed for GDGT-2, which had a distinct second maximum at 200 m at both NB and CB, and for the crenarchaeol isomer, for which concentrations were elevated over a broader range of depths at NB and CB, spanning ~100–200 m (Table 1).

3.4. TEX_{86} values and inferred temperatures

TEX_{86} was calculated according to Schouten et al. (2002) and ranged from 0.60 to 0.85 (Table 2). The surface waters of all three sites had the lowest TEX_{86}. TEX_{86} increased with depth from the top of the thermocline, reaching maximum values in the deeper subsurface between 150 and 200 m. TEX_{86} declined again below these depths at NB and CB (Fig. 4). TEX_{86}-inferred temperatures were calculated with the Castañeda and Schouten (2015) global lacustrine calibration:

$$T = 49.032 \times TEX_{86} - 10.989 \quad (r^2 = 0.88;\ n = 16)$$

The Castañeda and Schouten (2015) calibration is a combination and revision of the lacustrine calibrations from Powers et al. (2010) and Tierney et al. (2010), both of which include data from Lake Malawi in addition to other large African lakes. The dataset used for the calibration was limited to lakes with average surface temperatures >10 °C and BIT < 0.5, conditions that are consistent with modern Lake Malawi.

TEX_{86}-inferred temperatures deviate substantially from measured temperatures, exceeding the uncertainty of the calibration in many samples; differences between measured and calculated temperatures range from ~0.6–10.2 °C at NB, 1.4–7.13 °C at CB, and 2.1–6.0 °C at SB. Trends in the inferred temperature profiles follow trends in TEX_{86}, resulting in negative residuals of temperatures calculated from SPM in the surface and positive residuals of temperatures calculated from SPM in the deep subsurface (Fig. 5).

4. Discussion

4.1. Niche of Thaumarchaeota in the water column of Lake Malawi

IPLs are better indicators than CLs of living, or at least recently living, microbial communities because the labile polar head groups are susceptible to rapid degradation following cell death. IPL concentrations of the Thaumarchaeota biomarker crenarchaeol are thus expected to track active populations of Thaumarchaeota in the water column (e.g., Hurley et al., 2018). IPLs with glycosidic head groups – DH and MH – however, are stable enough as free lipids such that these compounds can accumulate in the water column and sediments (Lipp et al., 2008; Schouten et al., 2010; Liu et al., 2011; Lengger et al., 2013, 2014; Xie et al., 2014). In the Arabian Sea, for example, MH-GDGTs, and DH-GDGTs to a lesser degree, accumulate in the oxygen minimum zone over 700 m below the depth that the primary Thaumarchaeota population inhabits and represent a mixture of HPH-GDGT degradation products, fossil IPLs exported from the surface waters, and new IPLs produced by deep-dwelling archaeal clades (Schouten et al.,

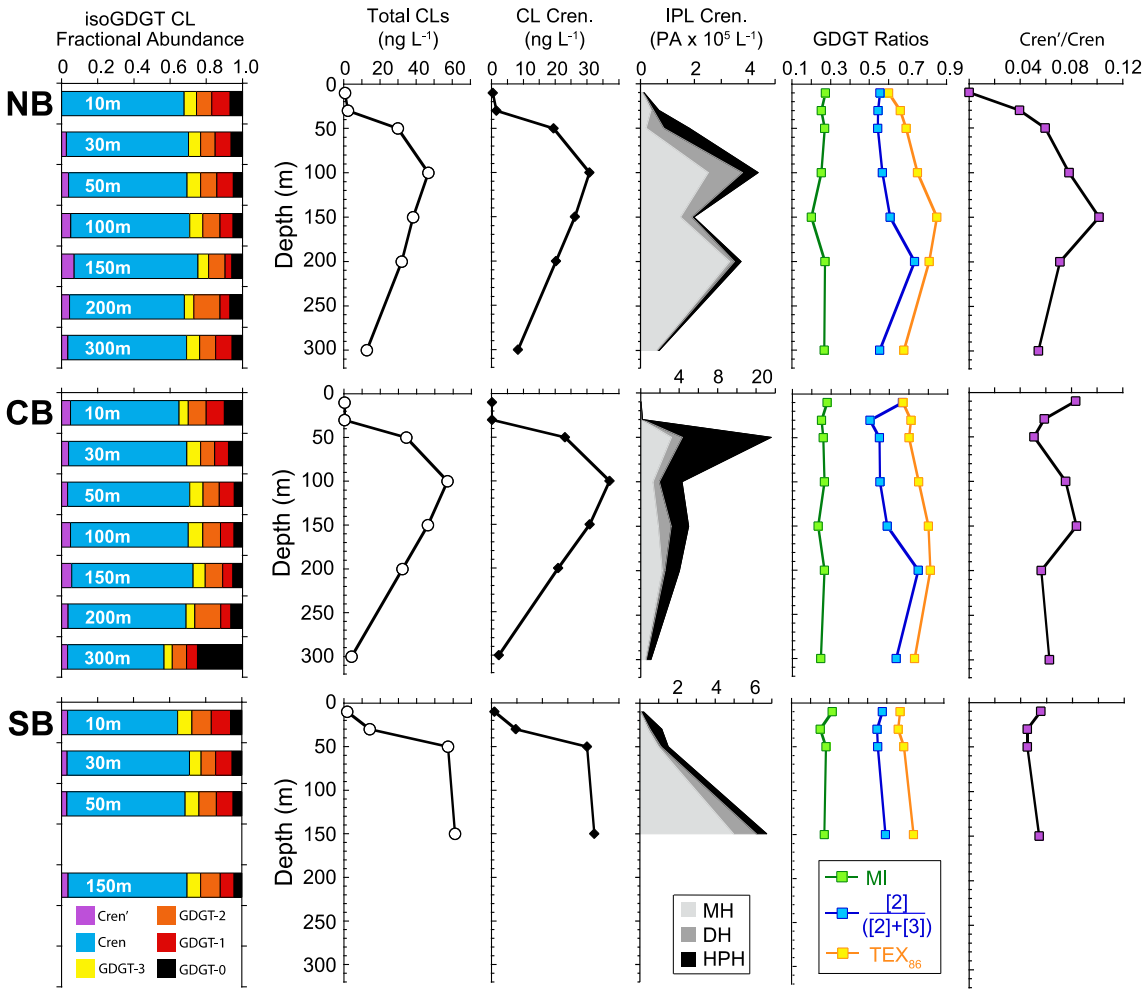

Fig. 4. Fractional abundances of CL iGDGTs at each sampling depth compared to profiles of total CL iGDGT, CL crenarchaeol, and IPL crenarchaeol concentrations. The MI (Methane Index), [2]/([2] + [3]), and Cren′/Cren ratio are intended to provide insights on the source of iGDGTs in the water column to explain observed trends in TEX_{86}.

Table 1
Concentration of iGDGT CLs and crenarchaeol IPLs in water column filtrates taken from Lake Malawi during Austral summer. Integers correspond to iGDGT structures in Fig. 1.

Depth (m)	0 (ng L^{-1})	1 (ng L^{-1})	2 (ng L^{-1})	3 (ng L^{-1})	Cren (ng L^{-1})	Cren′ (ng L^{-1})	HPH (PA L^{-1})	DH (PA L^{-1})	MH (PA L^{-1})
North basin site									
10	0.04	0.06	0.05	0.04	0.40	0.0	2.4E+3	5.5E+2	9.5E+3
30	0.14	0.20	0.18	0.15	1.5	0.06	2.0E+4	9.3E+3	3.9E+4
50	1.5	2.7	2.7	2.2	19.5	1.2	9.4E+4	6.6E+4	2.1E+4
100	2.4	3.4	4.4	3.4	30.7	2.4	5.8E+4	1.3E+5	2.5E+5
150	2.2	1.5	3.5	2.3	26.2	2.7	6.8E+3	4.2E+4	1.5E+5
200	2.2	1.8	4.6	1.7	20.3	1.4	2.5E+4	1.8E+4	3.3E+5
300	0.73	1.2	1.1	0.91	8.3	0.45	6.5E+3	1.8E+3	6.1E+4
Central basin site									
10	0.02	0.02	0.02	0.01	0.12	0.01	1.4E+2	2.2E+2	3.1E+3
30	0.02	0.02	0.02	0.02	0.17	0.01	6.4E+3	1.1E+4	1.4E+3
50	1.5	2.9	3.1	2.5	23.1	1.2	9.2E+5	1.1E+5	3.2E+5
100	2.7	4.2	5.6	4.6	37.1	2.8	2.4E+5	6.5E+4	1.3E+5
150	2.5	2.6	4.5	3.1	30.9	2.6	1.8E+5	1.3E+5	1.9E+5
200	2.1	1.8	4.6	1.6	20.9	1.2	1.5E+5	3.0E+4	2.2E+5
300	1.0	0.25	0.33	0.19	2.2	0.14	4.8E+4	6.3E+3	5.2E+4
South Basin site									
10	0.11	0.19	0.19	0.14	1.1	0.06	1.4E+4	2.7E+2	5.7E+3
30	0.76	1.3	1.1	0.92	9.5	0.43	6.3E+4	1.0E+4	4.4E+4
50	2.8	5.3	5.5	4.5	37.5	1.7	3.9E+4	1.5E+4	9.7E+4
150	2.6	4.6	6.6	4.6	40.3	2.2	5.6E+4	1.2E+5	5.0E+5

Table 2
iGDGT indices and calculated temperatures of CLs extracted from SPM in Lake Malawi.

Depth (m)	TEX_{86}	TEX_{86} inferred T[a]	TEX_{86}^{H} inferred T[b]	BIT Index	$\frac{GDGT\text{-}0}{Cren}$	$\frac{Cren'}{Cren}$	$\frac{[2]}{[2]+[3]}$
North basin site							
10	0.7	18.4	17.7	0.30	0.10	0.00	0.56
30	0.7	21.4	20.0	0.25	0.09	0.04	0.55
50	0.7	22.8	21.1	0.24	0.08	0.06	0.54
100	0.8	25.8	23.2	0.21	0.08	0.08	0.57
150	0.9	30.7	26.2	0.13	0.09	0.10	0.61
200	0.8	28.7	25.0	0.14	0.11	0.07	0.74
300	0.7	22.4	20.8	0.20	0.09	0.05	0.55
Central basin site							
10	0.7	21.9	20.4	0.33	0.17	0.08	0.67
30	0.7	21.4	20.0	0.35	0.12	0.06	0.50
50	0.7	23.3	21.5	0.26	0.07	0.05	0.55
100	0.8	25.8	23.2	0.24	0.07	0.08	0.55
150	0.8	28.2	24.7	0.15	0.08	0.08	0.59
200	0.8	28.7	25.0	0.12	0.10	0.06	0.75
300	0.7	24.3	22.2	0.39	0.47	0.06	0.63
South basin site							
10	0.7	22.4	20.8	0.25	0.10	0.06	0.58
30	0.7	21.4	20.0	0.17	0.08	0.05	0.55
50	0.7	22.8	21.1	0.23	0.07	0.05	0.55
150	0.7	25.3	22.8	0.17	0.07	0.05	0.59

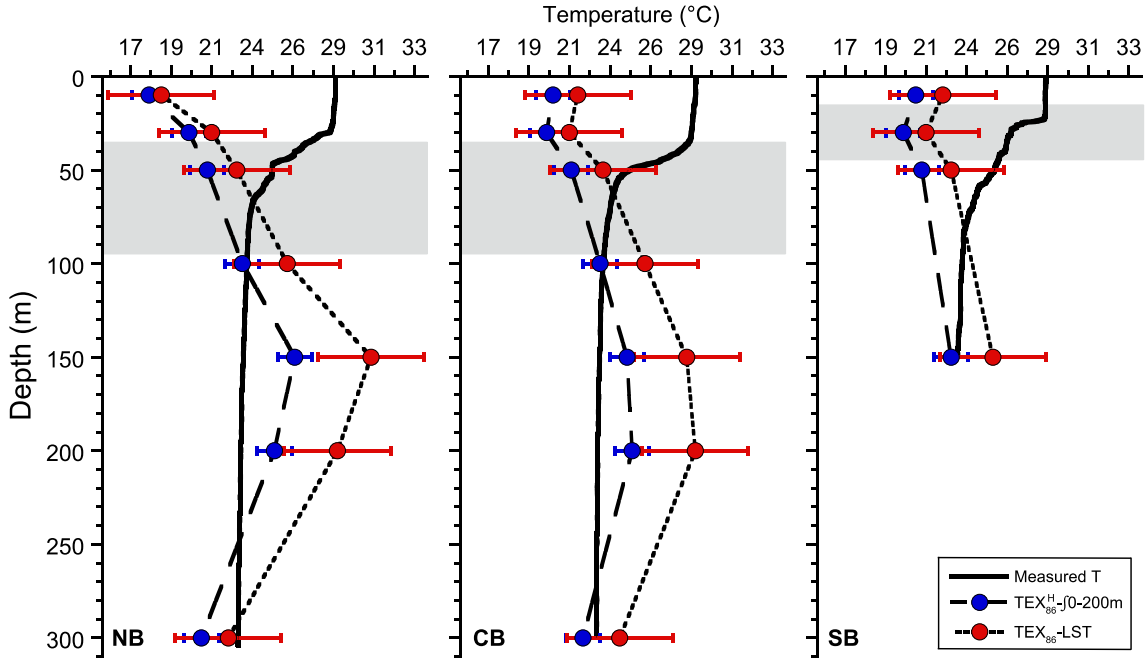

Fig. 5. Profiles of in situ water column temperatures and temperatures reconstructed from distributions of CL iGDGTs with two calibrations: The Castañeda and Schouten (2015) calibration is based on the TEX_{86} of globally distributed lacustrine surface sediments and LST, while the Kim et al. (2015) calibration is based on the TEX_{86}^{H} (TEX_{86}^{H} = log (TEX_{86})) of deep-water (>1000 m) sediments from the Mediterranean and Red Seas and the integrated upper water column temperatures (0–200 m) of the overlying surface waters. Error bars for each calibration reflect the root mean square errors reported in the respective studies, which is 3.1 °C for the Castañeda and Schouten (2015) calibration, and 1 °C for the Kim et al. (2015) calibration. Grey shading highlights the depths Group I.1a Thaumarchaeota were most likely inhabiting at the time of sampling based on HPH-crenarchaeol concentrations. (For interpretation of the references to colour in this figure legend, the reader is referred to the web version of this article.)

2012a). The deeper maxima of DH- and MH-crenarchaeol concentrations relative to HPH-crenarchaeol in Lake Malawi (Fig. 4) are consistent with such observations of iGDGT IPL abundances with depth in the marine water column. This suggests that the lipids are also derived from multiple sources, i.e. HPH-crenarchaeol degradation, new production, and vertical and/or lateral transport. The relative contribution of each of these processes to the total DH- and MH-crenarchaeol pool is difficult to ascertain without additional information, such as the isotopic composition of the lipids, and therefore cannot confidently be used as indicators of active Thaumarchaeota.

Conversely, HPH-crenarchaeol is highly specific to ammonia oxidizing archaea (AOA) and covaries with Thaumarchaeotal gene abundances in other environments (Pitcher et al., 2011a, 2011b; Schouten et al., 2012a; Buckles et al., 2013; Lipsewers et al., 2014; Sollai et al., 2018). HPH-crenarchaeol concentrations are also particularly suitable for tracking active Thaumarchaeota populations given that the compound can be up to 7 times more abundant during the growth phase compared to the stationary phase in cultures of the Thaumarchaeon *Nitrosopumilus maritimus* (Elling et al., 2014). It is unlikely that the sampling resolution employed for this study captured the precise depth of HPH-crenarchaeol maxima,

however it must be >30 m and <100 m water depth as we observe maximum concentrations ~50 m at both NB and CB, and ~30 m depth at SB (Fig. 4). *amo*A gene abundances provide an independent record of Thaumarchaeotal activity as it is an essential gene in AOA and demonstrated to be a robust indicator of Thaumarchaeota populations (Könneke et al., 2005; Wuchter et al., 2006; de la Torre et al., 2008; Pester et al., 2011; Stahl and de la Torre, 2012). Abundances of *amo*A genes and total archaeal 16S rRNA in the water column of Lake Malawi are both greatest at depths of 50 m at NB, at 30 m at SB, and at 50 m and 100 m, respectively, at CB (Muñoz-Ucros, 2014) and thus corroborate our interpretation of the HPH-crenarchaeol record. Muñoz-Ucros (2014) used an identical sampling scheme as the one employed in this study so likely also did not resolve the true maximum depth of *amo*A gene and archaeal 16S rRNA abundances. Nevertheless, it is clear that Thaumarchaeota across Lake Malawi resided within the upper 100 m of the water column near the base of the thermocline at the time of sampling.

The depth constraints imposed by the HPH-crenarchaeol and *amo*A gene records imply that Thaumarchaeota in Lake Malawi occupied a slightly different ecological niche during the study period than that of Thaumarchaeota in other stratified lacustrine systems. Thaumarchaeota metabolize ammonium so populations commonly reside where reduced nitrogen is abundant, generally near the redox boundary (e.g., Sinninghe Damsté et al., 2009; Llirós et al., 2010; Blaga et al., 2011; Schouten et al., 2012b; Woltering et al., 2012; Buckles et al., 2013; Kraemer et al., 2015; Zhang et al., 2011, 2016; Becker et al., 2018; Hurley et al., 2018). Studies of offshore nutrient abundances in Lake Malawi are sparse as most have focused on the littoral zones where the lake's fish populations, which are a crucial part of the local economy, are concentrated. The few studies (Bootsma and Hecky, 1999; Hamblin et al., 2003a) that have reported vertical profiles of pelagic nutrient abundances in Lake Malawi found maximum ammonium concentrations at the anoxic-oxic boundary during the austral winter, though no profiles during the summer season were presented in either study. As the vertical flux of ammonium from the anoxic hypolimnion into the upper 200 m of the lake is dominated by upwelling and turbulent mixing (Bootsma and Hecky, 1999; Guildford et al., 2000; Hamblin et al., 2003a), it is possible that ammonium is actually depleted in January relative to the winter months at the redox boundary as stratified conditions are well developed and new inputs of the nutrient from physical mixing processes are likely minimal (Guildford et al., 2000). This is even more likely at the northern reaches of the lake where upwelling is rare throughout the annual cycle (Hamblin et al., 2003a). Again, though no profiles representing NH_4^+ concentrations with depth in January are available, Hamblin et al. (2003a) did measure the NH_4^+ in the south basin near the location of SB in March, April, and May of 1997. The authors found concentrations were ~2–100 times lower between 0 and 100 m than 150 and 200 m in both March and April yet ~4 times greater at 50 m compared to 150–200 m in May following the onset of the winter mixing regime.

Thaumarchaeota populations growing in Lake Malawi during the austral summer months therefore may depend on alternative sources of ammonium. As such, the shallower than expected depths of Thaumarchaeota observed in this study could be related to the atmospheric deposition of nutrients, which can be a significant source of NH_4^+ during the austral summer (Bootsma et al., 1999). Whether enhanced atmospheric NH_4^+ deposition was a factor in driving a shoaling of Thaumarchaeota populations in January 2010 is difficult to conclude, however, as the interannual variability of atmospheric nitrogen deposition in Lake Malawi is poorly understood (Bootsma et al., 1999) and no measurements are available for the study period. Furthermore, Guildford et al. (2000) estimated that external nutrient inputs to Lake Malawi satisfied <15% of total demand. The nutrient supply in the upper oxic and suboxic layers of the lake is more typically dominated by recycling, with the rate of nutrient regeneration via remineralization as the primary limitation on microbial growth (Guildford et al., 2000).

Cyanobacteria are abundant in Lake Malawi during austral summer and can also provide a significant source of nitrogen to the lake through the fixation of atmospheric N_2 (Hecky and Kling, 1987; Bootsma and Hecky, 1999; Gondwe et al., 2008). Given the potentially very low concentrations of NH_4^+ at the redox boundary during this season, it is possible that the supply of bioavailable nitrogen generated through the decomposition of cyanobacterial biomass by heterotrophic bacteria sets up a gradient in nutrient concentrations that drives the vertical migration of Thaumarchaeotal populations. The abundance of Thaumarchaeota in the Eastern Pacific off the Southern California Bight varies seasonally and is likely related to changes in nutrient availability, as they have been shown to form synergistic consortia with heterotrophic bacteria that enhance the breakdown and recycling of nutrients at the base of the deep chlorophyll maximum (Jones and Hood, 1980; Beman et al., 2011). Given our observations of higher Thaumarchaeotal activity just below the deep chlorophyll maximum, it is possible that Thaumarchaeota in Lake Malawi exhibited similar behavior during the period in January sampled in this study. Nitrogen limitation can vary in the upper 60 m of Lake Malawi's water column on the order of days during the austral summer (Guildford et al., 2000), so concomitant studies of iGDGT production, nutrient concentrations, and microbial diversity are needed to determine whether the possible vertical migration of Thaumarchaeota is typical for the stratified season. Regardless, redox conditions do not appear to limit the vertical distribution of Thaumarchaeota or iGDGT production in Lake Malawi (Qin et al., 2015; Zhang et al., 2016).

4.2. Other archaeal communities in Lake Malawi

If CL crenarchaeol in the water column is primarily derived from the degradation of HPH-crenarchaeol produced by living Thaumarchaeota, maximum concentrations of CL crenarchaeol should occur just below the depth of maximum HPH-crenarchaeol abundances. CL crenarchaeol concentrations at all three of our sampling sites follow this expected pattern (Fig. 4). As HPH-crenarchaeol does not necessarily degrade directly to CL crenarchaeol, the intermediate degradation products DH- and MH-crenarchaeol would also accumulate at this depth. Indeed, at NB and SB, high concentrations of DH- and MH-crenarchaeol coincide with the depths of maximum CL crenarchaeol concentrations and therefore likely, in part, reflect the accumulation of lipids derived from the Thaumarchaeota population living above. This pattern does not hold at CB where DH- and MH-crenarchaeol peaks coincide with the HPH-crenarchaeol maxima rather than the maximum CL crenarchaeol concentrations (Fig. 4). It is possible that the degradation of all IPL crenarchaeol species is more rapid at CB than at NB or SB so that the glycosidic IPLs also do not accumulate in significant abundances below the depth of production. Alternatively, again, perhaps the actual highest abundances of these compounds occur at an intermediate depth that was unaccounted for with the sampling resolution employed in this study. A third explanation considers the limited time resolution of our study. It is possible that the depth of maximum Thaumarchaeotal activity observed at NB and SB is phenomenological and the average depth of habitat is closer to 100 m. Regardless, all three scenarios imply that high concentrations of CL iGDGTs and the more recalcitrant IPLs located within the thermocline are likely derived from active Thaumarchaeota inhabiting similar depths.

A conspicuous secondary peak in MH-crenarchaeol at 200 m at NB and CB (Fig. 4) requires further explanation. One of the

remarkable features in the profiles of CL distributions at NB and CB is an increase in the factional abundance of GDGT-2 relative to GDGT-3 also at 200 m. Increases in the ratio of GDGT-2/(GDGT-2 + GDGT-3) in the anoxic water column has been linked to populations of methanotrophs, methanogens, and non-Group I.1a Thaumarchaeota in other studies (Pancost et al., 2001; Blumenberg et al., 2004; Ingalls et al., 2006; Turich et al., 2007; Shah et al., 2008; Sintes et al., 2013; Taylor et al., 2013; Villanueva et al., 2014a) so it is necessary to explore the possibility that one or more of these groups inhabit Lake Malawi and may be contributing to the sedimentary iGDGT pool. Contributions of iGDGTs by methanotrophic archaea can be detected with the Methane Index (MI; Zhang et al., 2011), defined as

$$\mathrm{MI} = \frac{[\text{GDGT-1}]+[\text{GDGT-2}]+[\text{GDGT-3}]}{[\text{GDGT-1}]+[\text{GDGT-2}]+[\text{GDGT-3}]+[\text{Cren}]+[\text{Cren}']}$$

Greater proportions of GDGTs 1–3, universally produced by archaea, relative to crenarchaeol and its isomer (Liu et al., 2018; Sinninghe Damsté et al., 2018) results in higher MI (0.3–0.5). The converse distribution is associated with lower MI (<0.3) and is diagnostic of Thaumarchaeota. We observe no change in MI (Fig. 4) suggesting that methanotrophic archaea are not significant in Lake Malawi between 0 and 300 m. This is consistent with the lack of evidence for elevated sulfate concentrations at these depths that would be required to support methanotrophy (Kelly et al., 1987; Bootsma and Hecky, 2003). Sinninghe Damsté et al. (2009) similarly observed increases in the relative abundance of GDGT-2 in the anoxic subsurface of Lake Challa, Africa, and attributed the pattern to methanogenic Euryarchaeota living in the lake's subsurface. IGDGT distributions characteristic of methanogenic archaea are dominated by GDGT-0 with minor amounts of GDGT-1 and GDGT-2 and no crenarchaeol. Thaumarchaeota produce large quantities of crenarchaeol and little GDGT-0 such that the ratio of GDGT-0/crenarchaeol in Thaumarchaeota cultures is always <2 (Blaga et al., 2009; Naeher et al., 2014; Sinninghe Damsté et al., 2009; Zhang et al., 2016). GDGT-0/crenarchaeol is <2 for all SPM samples in Lake Malawi, eliminating the possibility of significant methanogenic populations in the subsurface (Table 2).

With no unequivocal evidence for methanogenic or methanotrophic Euryarchaeota, the elevated GDGT-2/(GDGT-2 + GDGT-3) in Malawi's anoxic subsurface likely corresponds to a deep-dwelling clade of Group I.1b Thaumarchaeota. The occupation of distinct vertical zones by the two Thaumarchaeotal groups is fairly common in both marine (Francis et al., 2005; De Corte et al., 2009; Hu et al., 2011, Hernández-Sánchez et al., 2014; Basse et al., 2014; Lengger et al., 2014; Kim et al., 2016) and lacustrine environments (Auguet et al., 2012; Buckles et al., 2013). Both groups belong to the Thaumarchaeota phylum, but Group I.1b does not produce iGDGTs with the same temperature relationship as Group I.1a Thaumarchaeota. Specifically, Group I.1b are associated with high proportions of the crenarchaeol isomer relative to crenarchaeol (Sinninghe Damsté et al., 2012b; Villanueva et al., 2014a; Kim et al., 2016; Elling et al., 2017). Abundances of the crenarchaeol isomer in Lake Malawi do in fact increase between 100 and 200 m at NB and CB (Table 2). Group I.1a Thaumarchaeota would produce lower quantities of the crenarchaeol isomer in response to the cooler water temperatures in the subsurface (Schouten et al., 2002; Elling et al., 2015) and there are no other known environmental factors that would induce abnormal production of the crenarchaeol isomer in this group. A population of Group I.1b Thaumarchaeota at NB and CB would further explain the increase in MH-crenarchaeol at this depth as chemotaxonomic analyses have shown that this group predominately produces IPLs with MH head groups (Elling et al., 2017). A metagenomic analysis conducted near CB in Lake Malawi found that Group I.1a Thaumarchaeota were significantly more diverse and abundant at thermocline depths ~100 m while genetic material from Group I.1b Thaumarchaeota was restricted to the deep subsurface ~300 m (Muñoz-Ucros, 2014), lending support for the presence of both groups of Thaumarchaeota in Lake Malawi. Notably, the CL and IPL data suggest the deeper dwelling clade resides closer to 150–200 m than 300 m, although this could be an artifact of the short time frame of the study. The importance of non-Group I.1a Thaumarchaeota at SB is less clear. Concentrations of GDGT-2 and the crenarchaeol isomer do increase below the surface (50–150 m) at this site, however the change is proportional to GDGT-3 and crenarchaeol, respectively, in contrast to observations in NB and CB (Table 2, Fig. 4). It is possible that Group I.1b Thaumarchaeota are present in the subsurface of SB, but the fully oxygenated water column characteristic of the shallow southern end of Lake Malawi prevents the populations that appear to prefer anoxic conditions at NB and CB from fully thriving.

4.3. TEX_{86} temperature profiles

With substantial evidence for multiple Thaumarchaeota populations in the water column of Lake Malawi, it is unsurprising that TEX_{86}-inferred temperature profiles are distinct from measured temperatures. Particularly interesting is that TEX_{86}-reconstructed temperatures are cooler than in situ temperatures in the surface, yet warmer than in situ temperatures in the deep subsurface (Fig. 5). Some studies have recently demonstrated that ammonia oxidation rates are inversely correlated to TEX_{86}, driving warm or cold biases in reconstructed temperatures depending on the relative dominance of shallow water or deep water Thaumarchaeota ecotypes – iGDGTs from shallow ecotypes inhabiting high-ammonium conditions result in a cold-bias and iGDGTs from deep ecotypes inhabiting low-ammonium conditions result in a warm-bias (Qin et al., 2015; Hurley et al., 2016, 2018). Zhang et al. (2016) also proposed that variable ammonium oxidation rates driven by redox conditions creates a negative correlation between DO concentrations and TEX_{86} in high latitude stratified lakes. As discussed above, the warm-bias in reconstructed temperatures from SPM in the deep subsurface is most likely due to the presence of a deep-dwelling Thaumarchaeota population, though the effect of low-ammonium conditions on iGDGT distributions cannot be ruled out.

The source of the cold-bias in reconstructed temperatures from the surface is less clear. Ammonium concentrations in the surface of Lake Malawi are low during austral summer (Guildford et al., 2000), but DO concentrations are high (Fig. 3) such that the net effect of the two parameters on TEX_{86} of SPM from the surface waters would be minimal if the CL pool is primarily derived from recently living Thaumarchaeota. Extremely low concentrations of HPH-crenarchaeol and all CL iGDGTs above 50 m at the time of sampling (Fig. 4), in addition to the presumably low concentrations of NH_4^+ in the surface waters, however, implies that in situ production of iGDGTs in the surface of Lake Malawi was low. Rather, TEX_{86} of surface water SPM could exhibit a cold-bias if the CL pool at these depths reflects iGDGTs produced during the austral winter. Surface water temperatures during the austral winter are only ~2 °C cooler than in the summer in Lake Malawi, still much warmer than reconstructed temperatures at these depths (Eccles 1974; Vollmer et al., 2005). Thaumarchaeota instead likely reside deeper in the water column during the austral winter to take advantage of the enhanced vertical flux of NH_4^+ at the redox boundary driven by turbulent mixing (Bootsma and Hecky, 1999; Guildford et al., 2000; Hamblin et al., 2003a). The effect of increased NH_4^+ fluxes on ammonia oxidation rates and ultimately iGDGT distributions coupled with the possible residence of Thaumarchaeota in the deeper, cooler waters near the redox boundary

may lead to the production of iGDGTs with a significant TEX_{86} cold-bias during austral winter. The anoxic-oxic interface is likely situated between 150 and 300 m during this season, though it would depend on the depth of the mixed layer (Bootsma and Hecky, 1999; Hamblin et al., 2003a). Annual average temperatures between 100 and 300 m are ~22 and 24 °C (Vollmer et al., 2005), similar to the TEX_{86}-reconstructed temperatures at the surface but still slightly warmer such that the effect of ammonium-oxidation rates on iGDGT distributions (Qin et al., 2015; Hurley et al., 2016, 2018) are necessary to fully explain the cold bias. Mixing of the upper 200 m of the water column driven by the strong southerly winds that persist from May to September could feasibly transport some of the iGDGTs produced at the redox boundary into the surface waters. While this explanation seems reasonable, a thorough investigation of iGDGT production and fluxes across multiple seasonal cycles is needed to validate these hypotheses.

The cold-bias is not as strong in SPM from the surface of CB and SB. The CL pools at these sites are likely additionally impacted by contributions of iGDGTs from the deep-dwelling Thaumarchaeota population based on elevated [GDGT-2]/([GDGT-2] + [GDGT-3]) and Cren′/Cren at the surface relative to the CL pools within the thermocline (Fig. 4). IGDGTs originally produced by the deep-dwelling Thaumarchaeota could also be transported to the surface during winter upwelling and would dampen the cold-bias in SPM TEX_{86} at these depths. As the northern end of the lake does not experience upwelling, and also perhaps receives less laterally transported material, the CL distributions in the surface at NB may only reflect iGDGTs produced locally in the mixed layer. However, again, a robust analysis of seasonal iGDGT fluxes throughout Lake Malawi is needed to support this idea. Overall, total CL iGDGT concentrations in the surface waters at the time of sampling were low across the lake, suggesting that the CL iGDGTs potentially transported to the surface from deeper within the water column do not accumulate substantially.

Interestingly, CLs in SPM sampled within the thermocline yielded reconstructed temperatures that are comparable to measured temperatures, at least within the range of uncertainty of the Castañeda and Schouten (2015) global lakes calibration (Fig. 5). Situated just below the depth of maximum Thaumarchaeota activity (Fig. 4), the CLs at these depths are likely derived from recently degraded IPL GDGTs (Hurley et al., 2018) and, conversely, unlikely to be derived from terrestrial sources or export of iGDGTs from the overlying surface waters as concentrations of CLs are two orders of magnitude lower in SPM above the thermocline (Fig. 4). If it is true that the thermocline-dwelling Thaumarchaeota form microbial consortia during this period to adapt to deep stratification and low nutrient availability, the potentially high NH_4^+/hypoxic microenvironments within the consortia (Paerl and Pinckney, 1996) may result in the production of iGDGT distributions with the expected relationship to in situ temperatures.

Core top sediments taken near NB have a TEX_{86} of 0.73 (Powers et al., 2004), remarkably similar to the range of TEX_{86} in SPM collected within the thermocline at the depths of maximum shallow-ecotype Thaumarchaeotal activity (~50–100 m) at NB (0.69–0.75). While this could be because iGDGT production during the austral summer dominates the export of CLs to the sediments, it could also be due to a sedimentary signal confounded by both iGDGTs produced during austral winter and by deep-ecotype Thaumarchaeota so as to appear similar to the values of thermocline iGDGTs from the study period. Polik et al. (2018) found that contributions of iGDGTs by deep-dwelling Thaumarchaeotal ecotypes to sedimentary distributions in the Mediterranean Sea were suppressed during periods of stratification. It is possible that the deep-ecotype Thaumarchaeota do not contribute significantly to the sedimentary CL pool given the strength of stratification of the upper water column in Lake Malawi, however further research is needed to better understand how the depth of habitat of Thaumarchaeota in Lake Malawi varies over the annual cycle, when maximum iGDGT production and export occurs, and if there is significant spatial variability in these processes, as these factors may additionally bias sedimentary distributions of iGDGTs.

Lastly, the relative contribution of iGDGTs by deep-dwelling Thaumarchaeota to the lake floor might vary considerably through time as lake levels and circulation regimes fluctuate (Filippi and Talbot, 2005). Though the principal mechanism that drives changes in the iGDGT composition of deep-dwelling Thaumarchaeota clades is still debated (Ingalls et al., 2006; Elling et al., 2015; Qin et al., 2015; Pearson et al., 2016; Becker et al., 2018; Hurley et al., 2018), Kim et al. (2015) found a significant relationship between iGDGT distributions in deep-water (>1000 m) sediments impacted by contributions from deep-dwelling Thaumarchaeota, evident by high relative abundances of GDGT-2 and the crenarchaeol isomer, and temperatures integrated over the upper 200 m of the overlying water column in the Mediterranean and Red Seas. As these are effectively large, restrictive basins and lipid abundances in SPM from the deep subsurface of Lake Malawi exhibit similar distributions to these deep-water sediments, it is possible that the temperature relationship developed by Kim et al. (2015) is applicable to Lake Malawi.

Furthermore, the MH-crenarchaeol profiles provide evidence that the deep-dwelling Thaumarchaeota in the lake reside ca. 150–200 m, so a correlation of deep water iGDGTs in Lake Malawi to temperatures integrated across the upper 200 m is expected. Indeed, the Kim et al. (2015) TEX_{86}^H calibration reduces the distance between calculated and measured temperatures in the deep subsurface, though there is still a slight warm-bias (Fig. 5). The calibration does not significantly improve temperatures calculated from shallow iGDGT distributions, highlighting its specific utility for tracking deep-water temperatures. Thus, while interpretations of TEX_{86} as a signal of upper water column temperatures are limited to sediments with low abundances of the crenarchaeol isomer and GDGT-2, information about the upper 200 m of the water column may still be derived when sedimentary iGDGT distributions reflect a mixture of shallow and deep-dwelling Thaumarchaeotal sources.

5. Conclusions

HPH-crenarchaeol abundances in SPM record maximum activity of Thaumarchaeota within the thermocline in the fully-oxygenated upper 100 m of Lake Malawi's water column. Increases in the relative abundances of GDGT-2, the CL crenarchaeol isomer, and MH-crenarchaeol in the deep subsurface indicate that Group I.1b Thaumarchaeota likely contributed to the CL GDGT pool at depths >150 m. The differences between measured and TEX_{86}-reconstructed temperatures in the subsurface at the time of sampling can therefore be attributed to production of iGDGTs by non-Group I.1a Thaumarchaeota. Production of iGDGTs by the surface-dwelling Thaumarchaeota, however, are an order of magnitude greater than the deeper clade and sedimentary TEX_{86} values appear to be dominated by upper water column distributions at least in the north basin, though more work is needed to evaluate the distributions and fluxes of iGDGTs produced during the austral winter. TEX_{86}-based temperatures associated with the depth of maximum GDGT production are within calibration error of in situ temperatures supporting the body of evidence that iGDGTs from active Group I.1a Thaumarchaeota populations record growth temperatures. An investigation of the depth of habitat of the surface-dwelling Thaumarchaeota throughout the annual cycle still needs to be conducted to fully understand the ecology of Thaumarchaeota in Lake Malawi and the timing of iGDGT production and export in Lake Malawi.

Acknowledgements

We give special thanks to Maxon Ngochera for his huge contributions in both organizing and assisting with this fieldwork on Lake Malawi. We also thank T.C. Johnson and R. Hecky for their help in organizing this research cruise on Lake Malawi, and T.C. Johnson additionally for providing the bathymetric data. We would like to thank the captain and crew of the R.V. Ndumduma, M. Berke, M. Maccuiane and A. Abbott for help they provided before, during, and after the cruise on Lake Malawi. We thank J. Ossebaar at the Royal NIOZ for their analytical assistance with IPLs. We thank two anonymous reviewers, Associate Editor P. Meyers, and the Editor-in-Chief J.K. Volkman for comments that improved this manuscript. This work was funded by grants from the National Geographic Society Committee for Research and Exploration (#8098-06) and University of Minnesota Grant-in-Aid of Research #20607 to JPW, and the University of Minnesota Office of International Programs to JPW and REH. A portion of this work was prepared while JPW was on leave at the Centre for Water Research, University of Western Australia, Crawley, WA, Australia and the WA-Organic and Isotope Geochemistry Centre, Curtin University of Technology, Bentley, WA, Australia. ECH, SS and JSSD are supported by the Netherlands Earth System Science Center (NESSC) funded by the Dutch ministry of Education, Culture and Science.

Appendix A. Supplementary material

Supplementary data to this article can be found online at https://doi.org/10.1016/j.orggeochem.2019.03.004.

Associate Editor—**Philip A. Meyers**

References

Auguet, J.C., Triadó-Margarit, X., Nomokonova, N., Camarero, L., Casamayor, E.O., 2012. Vertical segregation and phylogenetic characterization of ammonia-oxidizing Archaea in a deep oligotrophic lake. The ISME Journal 6, 1786–1797.

Basse, A., Zhu, C., Versteegh, G.J.M., Fischer, G., Hinrichs, K.-U., Mollenhauer, G., 2014. Distribution of intact and core tetraether lipids in water column profiles of suspended particulate matter off Cape Blanc, NW Africa. Organic Geochemistry 72, 1–13.

Beadle, L.C., 1981. The Inland Waters of Tropical Africa. Longman, London.

Bechtel, A., Smittenberg, R.H., Bernasconi, S.M., Schubert, C.J., 2010. Distribution of branched and isoprenoid tetraether lipids in an oligotrophic and a eutrophic Swiss lake: insights into sources and GDGT-based proxies. Organic Geochemistry 41, 822–832.

Becker, K.W., Elling, F.J., Schröder, J.M., Lipp, J.S., Goldhammer, T., Zabel, M., Elvert, M., Overmann, J., Hinrichs, K.U., 2018. Isoprenoid quinones resolve the stratification of redox processes in a biogeochemical continuum from the photic zone to deep anoxic sediments of the Black Sea. Applied and Environmental Microbiology 84, 1–20.

Beman, J.M., Steele, J.A., Fuhrman, J.A., 2011. Co-occurrence patterns for abundant marine archaeal and bacterial lineages in the deep chlorophyll maximum of coastal California. ISME Journal 5, 1077–1085.

Berke, M.A., Johnson, T.C., Werne, J.P., Grice, K., Schouten, S., Sinninghe Damsté, J.S., 2012a. Molecular records of climate variability and vegetation response since the Late Pleistocene in the Lake Victoria basin, East Africa. Quaternary Science Reviews 55, 59–74.

Berke, M.A., Johnson, T.C., Werne, J.P., Schouten, S., Sinninghe Damsté, J.S., 2012b. A mid-Holocene thermal maximum at the end of the African Humid Period. Earth and Planetary Science Letters 351, 95–104.

Berke, M.A., Johnson, T.C., Werne, J.P., Livingstone, D.A., Grice, K., Schouten, S., Sinninghe Damsté, J.S., 2014. Characterization of the last deglacial transition in tropical East Africa: Insights from Lake Albert. Palaeogeography, Palaeoclimatology, Palaeoecology 409, 11–18.

Blaga, C.I., Reichart, G.J., Heiri, O., Sinninghe Damsté, J.S., 2009. Tetraether membrane lipid distributions in water-column particulate matter and sediments: a study of 47 European lakes along a north-south transect. Journal of Paleolimnology 41, 523–540.

Blaga, C.I., Reichart, G.J., Vissers, E.W., Lotter, A.F., Anselmetti, F.S., Sinninghe Damsté, J.S., 2011. Seasonal changes in glycerol dialkyl glycerol tetraether concentrations and fluxes in a perialpine lake: implications for the use of the TEX_{86} and BIT proxies. Geochimica et Cosmochimica Acta 75, 6416–6428.

Bligh, E., Dyer, W.J., 1959. A rapid method of total lipid extraction and purification. Canadian Journal of Biochemistry and Physiology 37, 911–917.

Blumenberg, M., Seifert, R., Reitner, J., Pape, T., Michaelis, W., 2004. Membrane lipid patterns typify distinct anaerobic methanotrophic consortia. Proceedings of the National Academy of Sciences of the United States of America 101, 11111–11116.

Bootsma, H.A., Hecky, R.E., 2003. A comparative introduction to the biology and limnology of the African Great Lakes. Journal of Great Lakes Research 29, 3–18.

Bootsma, H.A., Hecky, R.E., 1999. Nutrient cycling in Lake Malawi/Nyasa Water Quality Report, Lake Malawi/Nyasa Biodiversity Conservation Project. SADC/GEF.

Bootsma, H.A., Mwita, J., Mwichande, B., Hecky, R.E., Kihedu, J., Mwambungu, J., 1999. The atmospheric deposition of nutrients on lake Malawi/Nyasa Water Quality Report for the SADC/GEF Lake Malawi/Nyasa Biodiversity Conservation Project. SADC/GEF, pp. 85–111.

Brochier-Armanet, C., Boussau, B., Gribaldo, S., Forterre, P., 2008. Mesophilic crenarchaeota: proposal for a third archaeal phylum, the Thaumarchaeota. Nature Reviews Microbiology 6, 245–252.

Buckles, L.K., Villanueva, L., Weijers, J.W.H., Verschuren, D., Sinninghe Damsté, J.S., 2013. Linking isoprenoidal GDGT membrane lipid distributions with gene abundances of ammonia-oxidizing Thaumarchaeota and uncultured crenarchaeotal groups in the water column of a tropical lake (Lake Challa, East Africa). Environmental Microbiology 15, 2445–2462.

Buckles, L.K., Weijers, J.W.H., Verschuren, D., Sinninghe Damsté, J.S., 2014. Sources of core and intact branched tetraether membrane lipids in the lacustrine environment: Anatomy of Lake Challa and its catchment, equatorial East Africa. Geochimica et Cosmochimica Acta 140, 106–126.

Castañeda, I.S., Schouten, S., 2015. Corrigendum to "A review of molecular organic proxies for examining modern and ancient lacustrine environments" [Quaternary Science Reviews 30 (2011) 2851–2891]. Quaternary Science Reviews 125, 174–176.

Castañeda, I.S., Schouten, S., 2011. A review of molecular organic proxies for examining modern and ancient lacustrine environments. Quaternary Science Reviews 30, 2851–2891.

De Corte, D., Yokokawa, T., Varela, M.M., Agogué, H., Herndl, G.J., 2009. Spatial distribution of Bacteria and Archaea and amoA gene copy numbers throughout the water column of the Eastern Mediterranean Sea. The ISME Journal 3, 147–158.

de la Torre, J.R., Walker, C.B., Ingalls, A.E., Könneke, M., Stahl, D.A., 2008. Cultivation of a thermophilic ammonia oxidizing archaeon synthesizing crenarchaeol. Environmental Microbiology 10, 810–818.

Eccles, D.H., 1974. An outline of the physical limnology of Lake Malawi (Lake Nyasa). Limnology and Oceanography 19, 730–742.

Elling, F.J., Könneke, M., Lipp, J.S., Becker, K.W., Gagen, E.J., Hinrichs, K.-U., 2014. Effects of growth phase on the membrane lipid composition of the thaumarchaeon Nitrosopumilus maritimus and their implications for archaeal lipid distributions in the marine environment. Geochimica et Cosmochimica Acta 141, 1579–1597.

Elling, F.J., Könneke, M., Mußmann, M., Greve, A., Hinrichs, K.-U., 2015. Influence of temperature, pH, and salinity on membrane lipid composition and TEX_{86} of marine planktonic thaumarchaeal isolates. Geochimica et Cosmochimica Acta 171, 238–255.

Elling, F.J., Könneke, M., Nicol, G.W., Stieglmeier, M., Bayer, B., Spieck, E., de la Torre, J.R., Becker, K.W., Thomm, M., Prosser, J.I., Herndl, G.J., Schleper, C., Hinrichs, K.U., 2017. Chemotaxonomic characterisation of the thaumarchaeal lipidome. Environmental Microbiology 19, 2681–2700.

Filippi, M.L., Talbot, M.R., 2005. The palaeolimnology of northern Lake Malawi over the last 25 ka based upon the elemental and stable isotopic composition of sedimentary organic matter. Quaternary Science Reviews 24, 1303–1328.

Francis, C.A., Roberts, K.J., Beman, J.M., Santoro, A.E., Oakley, B.B., 2005. Ubiquity and diversity of ammonia-oxidizing archaea in water columns and sediments of the ocean. Proceedings of the National Academy of Sciences of the United States of America 102, 14683–14688.

Gliozzi, A., Paoli, G., De Rosa, M., Gambacorta, A., 1983. Effect of isoprenoid cyclization on the transition temperature of lipids in thermophilic archaebacteria. Biochimica et Biophysica Acta – Biomembranes 735, 234–242.

Gondwe, M.J., Guildford, S.J., Hecky, R.E., 2008. Planktonic nitrogen fixation in Lake Malawi/Nyasa. Hydrobiologia 596, 251–267.

Guildford, S.J., Bootsma, H.A., Fee, E.J., Hecky, R.E., Patterson, G., 2000. Phytoplankton nutrient status and mean water column irradiance in Lakes Malawi and Superior. Aquatic Ecosystem Health and Management 3, 35–45.

Hamblin, P.F., Bootsma, H.A., Hecky, R.E., 2003a. Modeling nutrient upwelling in Lake Malawi/Nyasa. Journal of Great Lakes Research 29, 34–47.

Hamblin, P.F., Bootsma, H.A., Hecky, R.E., 2003b. Surface meteorological observations over Lake Malawi/Nyasa. Journal of Great Lakes Research 29 (Supplement), 19–33.

Hecky, R.E., Kling, H.J., 1987. Phytoplankton ecology of the Great Lakes in the Rift Valleys of Central Africa. Archiv für Hydrobiologie–BeiheftErgebnisse der. Limnologie 25, 197–228.

Hernández-Sánchez, M.T., Woodward, E.M.S., Taylor, K.W.R., Henderson, G., Pancost, R.D., 2014. Variations in GDGT distributions through the water column in the South East Atlantic Ocean. Geochimica et Cosmochimica Acta 132, 337–348.

Hu, A.Y., Jiao, N.Z., Zhang, R., Yang, Z., 2011. Niche partitioning of marine group I crenarchaeota in the euphotic and upper mesopelagic zones of the East China Sea. Applied and Environmental Microbiology 77, 7469–7478.

Huguet, C., Hopmans, E.C., Febo-Ayala, W., Thompson, D.H., Sinninghe Damsté, J.S., Schouten, S., 2006. An improved method to determine the absolute abundance

of glycerol dibiphytanyl glycerol tetraether lipids. Organic Geochemistry 37, 1036–1041.
Hurley, S.J., Elling, F.J., Könneke, M., Buchwald, C., Wankel, S.D., Santoro, A.E., Lipp, J. S., Hinrichs, K.-U., Pearson, A., 2016. Influence of ammonia oxidation rate on thaumarchaeal lipid composition and the TEX_{86} temperature proxy. Proceedings of the National Academy of Sciences of the United States of America 113, 7762–7767.
Hurley, S.J., Lipp, J.S., Close, H.G., Hinrichs, K.U., Pearson, A., 2018. Distribution and export of isoprenoid tetraether lipids in suspended particulate matter from the water column of the Western Atlantic Ocean. Organic Geochemistry 116, 90–102.
Ingalls, A.E., Shah, S.R., Hansman, R.L., Aluwihare, L.I., Santos, G.M., Druffel, E.R.M., Pearson, A., 2006. Quantifying archaeal community autotrophy in the mesopelagic ocean using natural radiocarbon. Proceedings of the National Academy of Sciences of the United States of America 103, 6442–6447.
Johnson, T.C., Davis, T.W., 1989. High resolution seismic profiles from Lake Malawi, Africa. Journal of African Earth Sciences (and the Middle East) 8, 383–392.
Johnson, T.C., Werne, J.P., Brown, E.T., Abbott, A., Berke, M.A., Steinman, B.A., Halbur, J., Contreras, S., Grosshuesch, S., Deino, A., Scholz, C.A., Lyons, R.P., Schouten, S., Sinninghe Damsté, J.S., 2016. A progressively wetter climate in southern East Africa over the past 1.3 million years. Nature 537, 220–224.
Jones, R.D., Hood, M.A., 1980. Interaction between an ammonium-oxidizer, *Nitrosomonas* sp., and two heterotrophic bacteria, *Nocardia atlantica* and *Pseudomonas* sp.: A note. Microbial Ecology 6, 271–275.
Kelly, A.C.A., Rudd, J.W.M., Hesslein, R.H., Schindler, D.W., Dillon, P.J., Gherini, S.A., Hecky, R.E., 1987. Prediction of biological acid neutralization in acid-sensitive lakes. Biogeochemistry 3, 129–140.
Kim, J.H., Schouten, S., Rodrigo-Gámiz, M., Rampen, S., Marino, G., Huguet, C., Helmke, P., Buscail, R., Hopmans, E.C., Pross, J., Sangiorgi, F., Middelburg, J.B.M., Sinninghe Damsté, J.S., 2015. Influence of deep-water derived isoprenoid tetraether lipids on the TEX_{86}^{H} paleothermometer in the Mediterranean Sea. Geochimica et Cosmochimica Acta 150, 125–141.
Kim, J.H., Villanueva, L., Zell, C., Sinninghe Damsté, J.S., 2016. Biological source and provenance of deep-water derived isoprenoid tetraether lipids along the Portuguese continental margin. Geochimica et Cosmochimica Acta 172, 177–204.
Könneke, M., Bernhard, A.E., de la Torre, J.R., Walker, C.B., Waterbury, J.B., Stahl, D.A., 2005. Isolation of an autotrophic ammonia-oxidizing marine archaeon. Nature 437, 543–546.
Kraemer, B.M., Hook, S., Huttula, T., Kotilainen, P., O'Reilly, C.M., Peltonen, A., Plisnier, P.D., Sarvala, J., Tamatamah, R., Vadeboncoeur, Y., Wehrli, B., McIntyre, P.B., 2015. Century-long warming trends in the upper water column of Lake Tanganyika. PLoS ONE 10, 1–17.
Lengger, S.K., Hopmans, E.C., Sinninghe Damsté, J.S., Schouten, S., 2014. Fossilization and degradation of archaeal intact polar tetraether lipids in deeply buried marine sediments (Peru Margin). Geobiology 12, 212–220.
Lengger, S.K., Kraaij, M., Tjallingii, R., Baas, M., Stuut, J.B., Hopmans, E.C., Sinninghe Damsté, J.S., Schouten, S., 2013. Differential degradation of intact polar and core glycerol dialkyl glycerol tetraether lipids upon post-depositional oxidation. Organic Geochemistry 65, 83–93.
Lipp, J.S., Hinrichs, K.-U., 2009. Structural diversity and fate of intact polar lipids in marine sediments. Geochimica et Cosmochimica Acta 73, 6816–6833.
Lipp, J.S., Morono, Y., Inagaki, F., Hinrichs, K.U., 2008. Significant contribution of Archaea to extant biomass in marine subsurface sediments. Nature 454, 991–994.
Lipsewers, Y.A., Bale, N.J., Hopmans, E.C., Schouten, S., Sinninghe Damsté, J.S., Villanueva, L., 2014. Seasonality and depth distribution of the abundance and activity of ammonia oxidizing microorganisms in marine coastal sediments (North Sea). Frontiers in Microbiology 5, 1–12.
Liu, X., Lipp, J.S., Hinrichs, K.U., 2011. Distribution of intact and core GDGTs in marine sediments. Organic Geochemistry 42, 368–375.
Liu, X.L., Lipp, J.S., Birgel, D., Summons, R.E., Hinrichs, K.U., 2018. Predominance of parallel glycerol arrangement in archaeal tetraethers from marine sediments: Structural features revealed from degradation products. Organic Geochemistry 115, 12–23.
Llirós, M., Gich, F., Plasencia, A., Auguet, J.C., Darchambeau, F., Casamayor, E.O., Descy, J.-P., Borrego, C., 2010. Vertical distribution of ammonia-oxidizing crenarchaeota and methanogens in the epipelagic waters of Lake Kivu (Rwanda-Democratic Republic of the Congo). Applied and Environmental Microbiology 76, 6853–6863.
Morrissey, A., Scholz, C.A., Russell, J.M., 2018. Late Quaternary TEX_{86} paleotemperatures from the world's largest desert lake, Lake Turkana, Kenya. Journal of Paleolimnology 59, 103–117.
Muñoz-Ucros, J., 2014. Planktonic archaeal diversity and ammonia-oxidizer abundance change with depth in Lakes Malawi, Kivu, and Superior. MS Thesis, University of Minnesota.
Naeher, S., Peterse, F., Smittenberg, R.H., Niemann, H., Zigah, P.K., Schubert, C.J., 2014. Sources of glycerol dialkyl glycerol tetraethers (GDGTs) in catchment soils, water column and sediments of Lake Rotsee (Switzerland) – Implications for the application of GDGT-based proxies for lakes. Organic Geochemistry 66, 164–173.
Paerl, H.W., Pinckney, J.L., 1996. A mini-review of microbial consortia: Their roles in aquatic production and biogeochemical cycling. Microbial Ecology 31, 225–247.
Pancost, R.D., Hopmans, E.C., Sinninghe Damsté, J.S., 2001. Archaeal lipids in mediterranean cold seeps: Molecular proxies for anaerobic methane oxidation. Geochimica et Cosmochimica Acta 65, 1611–1627.
Pearson, A., Hurley, S.J., Walter, S.R.S., Kusch, S., Lichtin, S., Zhang, Y.G., 2016. Stable carbon isotope ratios of intact GDGTs indicate heterogeneous sources to marine sediments. Geochimica et Cosmochimica Acta 181, 18–35.
Pester, M., Schleper, C., Wagner, M., 2011. The Thaumarchaeota: An emerging view of their phylogeny and ecophysiology. Current Opinion in Microbiology 14, 300–306.
Pitcher, A.M., Hopmans, E.C., Mosier, A.C., Park, S.J., Rhee, S.K., Francis, C.A., Schouten, S., Sinninghe Damsté, J.S., 2011a. Core and intact polar glycerol dibiphytanyl glycerol tetraether lipids of ammonia-oxidizing Archaea enriched from marine and estuarine sediments. Applied and Environmental Microbiology 77, 3468–3477.
Pitcher, A.M., Villanueva, L., Hopmans, E.C., Schouten, S., Reichart, G.J., Sinninghe Damsté, J.S., 2011b. Niche segregation of ammonia-oxidizing archaea and anammox bacteria in the Arabian Sea oxygen minimum zone. ISME Journal 5, 1896–1904.
Polik, C.A., Elling, F.J., Pearson, A., 2018. Impacts of paleoecology on the TEX_{86} sea surface temperature proxy in the Pliocene-Pleistocene Mediterranean Sea. Paleoceanography and Paleoclimatology 33, 1472–1489.
Powers, L.A., Johnson, T.C., Werne, J.P., Castañeda, I.S., Hopmans, E.C., Sinninghe Damsté, J.S., Schouten, S., 2011. Organic geochemical records of environmental variability in Lake Malawi during the last 700 years, Part I: The TEX_{86} temperature record. Palaeogeography, Palaeoclimatology, Palaeoecology 303, 133–139.
Powers, L.A., Johnson, T.C., Werne, J.P., Castañeda, I.S., Hopmans, E.C., Sinninghe Damsté, J.S., Schouten, S., 2005. Large temperature variability in the southern African tropics since the Last Glacial Maximum. Geophysical Research Letters 32, 1–4.
Powers, L.A., Werne, J.P., Johnson, T.C., Hopmans, E.C., Sinninghe Damsté, J.S., Schouten, S., 2004. Crenarchaeotal membrane lipids in lake sediments: A new paleotemperature proxy continental paleoclimate reconstruction? Geology 32, 613–616.
Powers, L.A., Werne, J.P., Vanderwoude, A.J., Sinninghe Damsté, J.S., Hopmans, E.C., Schouten, S., 2010. Applicability and calibration of the TEX_{86} paleothermometer in lakes. Organic Geochemistry 41, 404–413.
Qin, W., Carlson, L.T., Armbrust, E.V., Devol, A.H., Moffett, J.W., Stahl, D.A., Ingalls, A. E., 2015. Confounding effects of oxygen and temperature on the TEX_{86} signature of marine Thaumarchaeota. Proceedings of the National Academy of Sciences of the United States of America 112, 10979–10984.
Schouten, S., Hopmans, E.C., Schefuß, E., Sinninghe Damsté, J.S., 2002. Distributional variations in marine crenarchaeotal membrane lipids: A new tool for reconstructing ancient sea water temperatures? Earth and Planetary Science Letters 204, 265–274.
Schouten, S., Hopmans, E.C., Sinninghe Damsté, J.S., 2013. The organic geochemistry of glycerol dialkyl glycerol tetraether lipids: A review. Organic Geochemistry 54, 19–61.
Schouten, S., Huguet, C., Hopmans, E.C., Kienhuis, M.V.M., Sinninghe Damsté, J.S., 2007. Analytical methodology for TEX_{86} paleothermometry by high-performance liquid chromatography/atmospheric pressure chemical ionization-mass spectrometry. Analytical Chemistry 79, 2940–2944.
Schouten, S., Middelburg, J.J., Hopmans, E.C., Sinninghe Damsté, J.S., 2010. Fossilization and degradation of intact polar lipids in deep subsurface sediments: A theoretical approach. Geochimica et Cosmochimica Acta 74, 3806–3814.
Schouten, S., Pitcher, A., Hopmans, E.C., Villanueva, L., van Bleijswijk, J., Sinninghe Damsté, J.S., 2012a. Intact polar and core glycerol dibiphytanyl glycerol tetraether lipids in the Arabian Sea oxygen minimum zone: I. Selective preservation and degradation in the water column and consequences for the TEX_{86}. Geochimica et Cosmochimica Acta 98, 228–243.
Schouten, S., Rijpstra, W.I.C., Durisch-Kaiser, E., Schubert, C.J., Sinninghe Damsté, J. S., 2012b. Distribution of glycerol dialkyl glycerol tetraether lipids in the water column of Lake Tanganyika. Organic Geochemistry 53, 34–37.
Shah, S.R., Mollenhauer, G., Ohkouchi, N., Eglinton, T.I., Pearson, A., 2008. Origins of archaeal tetraether lipids in sediments: insights from radiocarbon analysis. Geochimica et Cosmochimica Acta 72, 4577–4594.
Sinninghe Damsté, J.S., Hopmans, E.C., Schouten, S., van Duin, A.C.T., Geenevasen, J. A.J., 2002. Crenarchaeol: the characteristic core glycerol dibiphytanyl glycerol tetraether membrane lipid of cosmopolitan pelagic crenarchaeota. Journal of Lipid Research 43, 1641–1651.
Sinninghe Damsté, J.S., Ossebaar, J., Abbas, B., Schouten, S., Verschuren, D., 2009. Fluxes and distribution of tetraether lipids in an equatorial African lake: constraints on the application of the TEX_{86} palaeothermometer and BIT index in lacustrine settings. Geochimica et Cosmochimica Acta 73, 4232–4249.
Sinninghe Damsté, J.S., Ossebaar, J., Schouten, S., Verschuren, D., 2012a. Distribution of tetraether lipids in the 25-ka sedimentary record of Lake Challa: extracting reliable TEX_{86} and MBT/CBT palaeotemperatures from an equatorial African lake. Quaternary Science Reviews 50, 43–54.
Sinninghe Damsté, J.S., Rijpstra, W.I.C., Hopmans, E.C., den Uijl, M.J., Weijers, J.W.H., Schouten, S., 2018. The enigmatic structure of the crenarchaeol isomer. Organic Geochemistry 124, 22–28.
Sinninghe Damsté, J.S., Rijpstra, W.I.C., Hopmans, E.C., Jung, M.Y., Kim, J.G., Rhee, S. K., Stieglmeier, M., Schleper, C., 2012b. Intact polar and core glycerol dibiphytanyl glycerol tetraether lipids of group I.1a and I.1b Thaumarchaeota in soil. Applied and Environmental Microbiology 78, 6866–6874.
Sintes, E., Bergauer, K., De Corte, D., Yokokawa, T., Herndl, G.J., 2013. Archaeal amoA gene diversity points to distinct biogeography of ammonia-oxidizing Crenarchaeota in the ocean. Environmental Microbiology 15, 1647–1658.

Sollai, M., Villanueva, L., Hopmans, E.C., Reichart, G.-J., Sinninghe Damsté, J.S., 2018. A combined lipidomic and 16S rRNA gene amplicon sequencing approach reveals archaeal sources of intact polar lipids in the stratified Black Sea water column. Geobiology. https://doi.org/10.1111/gbi.12316.

Spang, A., Hatzenpichler, R., Brochier-Armanet, C., Rattei, T., Tischler, P., Spieck, E., Streit, W., Stahl, D.A., Wagner, M., Schleper, C., 2010. Distinct gene set in two different lineages of ammonia-oxidizing archaea supports the phylum Thaumarchaeota. Trends in Microbiology 18, 331–340.

Stahl, D.A., de la Torre, J.R., 2012. Physiology and diversity of ammonia-oxidizing archaea. Annual Review of Microbiology 66, 83–101.

Sturt, H.F., Summons, R.E., Smith, K., Elvert, M., Hinrichs, K.-U., 2004. Intact polar membrane lipids in prokaryotes and sediments deciphered by high-performance liquid chromatography/electrospray ionization multistage mass spectrometry – New biomarkers for biogeochemistry and microbial ecology. Rapid Communications in Mass Spectrometry 18, 617–628.

Taylor, K.W.R., Huber, M., Hollis, C.J., Hernández-Sánchez, M.T., Pancost, R.D., 2013. Re-evaluating modern and Palaeogene GDGT distributions: Implications for SST reconstructions. Global and Planetary Change 108, 158–174.

Tierney, J.E., Mayes, M.T., Meyer, N., Johnson, C., Swarzenski, P.W., Cohen, A.S., Russell, J.M., 2010. Late-twentieth-century warming in Lake Tanganyika unprecedented since AD 500. Nature Geoscience 3, 422–425.

Tierney, J.E., Russell, J.M., Huang, Y., Sinninghe Damsté, J.S., Hopmans, E.C., Cohen, A. S., 2008. Northern Hemisphere controls on tropical southeast African Climate during the past 60,000 years. Science 322, 252–255.

Turich, C., Freeman, K.H., Bruns, M.A., Conte, M., Jones, A.D., Wakeham, S.G., 2007. Lipids of marine Archaea: patterns and provenance in the water-column and sediments. Geochimica et Cosmochimica Acta 71, 3272–3291.

Villanueva, L., Schouten, S., Sinninghe Damsté, J.S., 2014a. Depth-related distribution of a key gene of the tetraether lipid biosynthetic pathway in marine Thaumarchaeota. Environmental Microbiology 17, 3527–3539.

Villanueva, L., Sinninghe Damsté, J.S., Schouten, S., 2014b. A re-evaluation of the archaeal membrane lipid biosynthetic pathway. Nature Reviews Microbiology 12, 438–448.

Vollmer, M.K., Weiss, R.F., Bootsma, H.A., 2002. Ventilation of Lake Malawi/Nyasa. In: Odada, E.O., Olago, D.O. (Eds.), The East African Great Lakes: Limnology, Palaeolimnology and Biodiversity. Advances in Global Change Research, vol. 12. Springer, Dordrecht.

Vollmer, M.K., Bootsma, H.A., Hecky, R.E., Patterson, G., Halfman, J.D., Edmond, J.M., Eccles, D.H., Weiss, R.F., 2005. Deep-water warming trend in Lake Malawi, East Africa. Limnology and Oceanography 50, 727–732.

Woltering, M., Johnson, T.C., Werne, J.P., Schouten, S., Sinninghe Damsté, J.S., 2011. Late Pleistocene temperature history of Southeast Africa: a TEX_{86} temperature record from Lake Malawi. Palaeogeography, Palaeoclimatology, Palaeoecology 303, 93–102.

Woltering, M., Werne, J.P., Kish, J.L., Hicks, R., Sinninghe Damsté, J.S., Schouten, S., 2012. Vertical and temporal variability in concentration and distribution of thaumarchaeotal tetraether lipids in Lake Superior and the implications for the application of the TEX_{86} temperature proxy. Geochimica et Cosmochimica Acta 87, 136–153.

Wuchter, C., Abbas, B., Coolen, M.J.L., Herfort, L., Timmers, P., Strous, M., Van Bleijswijk, J., Teira, E., Herndl, G.J., Middelburg, J.J., Schouten, S., Sinninghe Damsté, J.S., 2006. Archaeal nitrification in the ocean. Proceedings of the National Academy of Sciences of the United States of America 103, 12317–12322.

Wuchter, C., Schouten, S., Coolen, M.J.L., Sinninghe Damsté, J.S., 2004. Temperature-dependent variation in the distribution of tetraether membrane lipids of marine Crenarchaeota: implications for TEX_{86} paleothermometry. Paleoceanography 19, 1–10.

Xie, S., Liu, X.L., Schubotz, F., Wakeham, S.G., Hinrichs, K.U., 2014. Distribution of glycerol ether lipids in the oxygen minimum zone of the Eastern Tropical North Pacific Ocean. Organic Geochemistry 71, 60–71.

Zhang, Y.G., Zhang, C.L., Liu, X.L., Li, L., Hinrichs, K.-U., Noakes, J.E., 2011. Methane index: a tetraether archaeal lipid biomarker indicator for detecting the instability of marine gas hydrates. Earth Planetary Science Letters 307, 525–534.

Zhang, Z., Smittenberg, R.H., Bradley, R.S., 2016. GDGT distribution in a stratified lake and implications for the application of TEX_{86} in paleoenvironmental reconstructions. Scientific Reports 6, 34465.